PAPER

Check for updates

Enhanced sensitivity and stability of wearable temperature sensors: a novel approach using inkjet printing†

Milad Ghalamboran,*[a,b] Judith Castillo-Rodriguez,*[a] Camille Anne Javonillo,[a] Sina Tahbaz,[a] Bryan Koivisto,*[c] Gerd Grau*[b] and Parnian Majd[a]

This work presents a wearable temperature sensor fabricated by inkjet printing using poly(3,4 ethylenedioxythiophene):poly(styrenesulfonate) (PEDOT:PSS) ink, with a top layer of extrusion-printed silver ink serving as electrodes, on both glass and cotton-based fabric substrates. PEDOT:PSS, a widely used conductive polymer, was selected due to its affordability, conductivity, and biocompatibility. The sensors demonstrated excellent humidity resistance with enhanced conductivity, making them ideal for wearable technology applications. The glass-based benchmark sensor exhibited a resistance change of approximately 30% across a temperature range of 23 to 40 °C, with sensitivity exceeding 1.7% per °C. In comparison, the fabric-based sensor, designed for wearable applications, showed a 20% decrease in resistance with sensitivity greater than 0.65% per °C. This represents a notable enhancement compared to values reported in the literature. Both sensors exhibited a strong linear relationship between temperature and resistance, with coefficients of determination (R^2) of 0.995 and 0.779 for the glass and fabric sensors, respectively. These results highlight the potential of fabric-integrated sensors for wearable applications, offering reliable performance and temperature sensitivity comparable to those of traditional glass-based sensors.

Introduction

Wearable technology has been revolutionary in recent years, offering remarkable advancements. With the increasing popularity of wearable activity-tracking devices, monitoring daily physical activity and promoting a healthy lifestyle has become more straightforward.[1–3] Smart wear has revolutionized the fashion industry by integrating technology with textiles, transforming the way we interact with our clothing and environment. The flexibility, comfort, and wearability of these devices allow for easier recording of any physical or chemical changes, all at an affordable price.[4,5]

One of the most important biomarkers is basal temperature, with temperature being one of the few vital parameters of the human body controlled by homeostasis.[6,7] Any changes in body temperature can indicate infections, inflammation, antigenic immune responses and treatment efficacy.[8] When

measuring, there are numerous types of thermometers that can be used, ranging from glass to infrared thermometers, with the rectal thermometer being most accurate in measurements.[9] However, the response of certain thermometers can be affected by environmental changes, and their invasiveness on the user can determine their usage level. To combat the limitations of existing technologies, a non-invasive wearable temperature sensor is proposed herein, designed to minimize environmental interference and enable continuous monitoring through simple skin contact. The skin, being the largest organ of the human body, plays a crucial role in thermoregulation by transmitting temperature changes *via* blood flow, typically within a range of 33–42 °C.[10–12] For reliable measurements, sensors must remain flexible, comfortable, and in constant contact with the skin.[13]

However, many current wearable sensors face significant challenges: some are not biocompatible,[14] causing irritation or discomfort over prolonged use; others are not cost-effective[15] or washable,[16] limiting their practicality for everyday wear; and some rely on optical infrared sensors, which are complex to integrate into wearable products and can suffer from inaccuracies due to environmental factors. Textile technologies have evolved to reduce costs and production times while enhancing flexibility and comfort, making real-time temperature monitoring more feasible. This work leverages these advancements by developing a fabric-based sensor that is light weight and suit-

[a]Fibra Inc., 44 Gerrard St E, Rm 303, Toronto, ON, M5B 1G3, Canada.
E-mail: miladgh@yorku.ca
[b]Department of Electrical Engineering and Computer Science, Lassonde School of Engineering, York University, 4700 Keele Street, Toronto, ON M3J 1P3, Canada
[c]Toronto Metropolitan University, Department of Chemistry and Biology, 350 Victoria St., Toronto, ON M5B 2K3, Canada
†Electronic supplementary information (ESI) available. See DOI: https://doi.org/10.1039/d5lp00036j
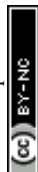
able for repeated washing, offering a practical and reliable solution for continuous temperature monitoring and integration into textile wearable applications.

In textile manufacturing, two prominent printing methods are used: extrusion printing and inkjet printing. Extrusion printing is favoured due to its ability to deposit thick, continuous layers of material, making it suitable for creating durable conductive traces. Inkjet printing, on the other hand, allows for precise patterning of fine features with minimal material usage, enabling high-resolution designs and reducing waste. Both methods have contributed to enhancing the efficiency of fabrication processes by optimizing material deposition, reducing production time, and enabling the integration of functional materials into textiles.[17,18] Extrusion printing involves the highly precise deposition of a material that continuously flows through a nozzle onto a substrate.[13–15] Alternatively, inkjet printing involves the ejection of non-viscous microdroplets onto a substrate.[14] Although both methods provide efficient customization, their mechanisms and applications greatly differ. Extrusion printing focuses on the formation of thick films with a resistivity of a few hundred $k\Omega$ cm^{-1}, but with low sheet resistance.[14,15] Inkjet printing uses a variety of inks with high solubility and low viscosity (less than 100 mPa s), which increase printing resolution.[18,19]

Development of these textile sensors utilizes ink consisting mostly of silver, carbon allotropes and polymers.[20] Poly(3,4-ethylenedioxythiophene):poly(styrenesulfonate) (PEDOT:PSS) is one of the popular polymers used in the last two decades due to its low cost, conductivity, solubility, flexibility, biocompatibility and ability to couple and transport ionic and electronic charges.[21–23] To further enhance the properties of PEDOT:PSS, implementation of cross-linkers leads to stabilized films for better adhesion, reducing redispersion, as well as influencing its electrical properties.[16,20] A methoxysilane-based molecule, such as (3-glycidyloxypropyl)trimethoxysilane (GOPS), is cross-linked with PEDOT:PSS to enhance aqueous stability and prevent dissolution and delamination of the polymer, making it suitable for use in humid environments.[16,24–26] The cross-linkage is accomplished by cross-linking GOPS with the hydrophilic section of the PSS unit in the outer shell of the PEDOT:PSS grain, enhancing grain boundary and reducing charge carrier mobility and conductivity.[16,26]

Recent advancements in temperature sensors for wearable applications have leveraged materials and fabrication methods to enhance flexibility, stability, and sensitivity. For instance, the use of reduced graphene oxide (rGO) and carbon nanotubes has enabled the development of flexible and stretchable temperature sensors, mimicking the properties of human skin to achieve high sensitivity and durability under mechanical deformation, with reported TCR values of approximately 0.0018 K^{-1} and 1.5×10^{-3} K^{-1}, respectively.[27,28] Additionally, inkjet printing processes on flexible substrates have been explored to realize low-cost and scalable production of temperature sensors, achieving reliable performance under varying environmental conditions, with a TCR of around 0.0025 K^{-1}.[29] The integration of these novel materials and fabrication tech-

niques demonstrates significant potential in healthcare and wearable electronics, offering precise temperature monitoring with improved user comfort and device longevity.[30,31]

In this paper, from the well-known use of PEDOT:PSS as the main active component, we introduce a novel and stable temperature-sensitive wearable sensor deposited onto a fabric substrate. We implemented inkjet printing using modified PEDOT:PSS as the base ink, which was placed into a rectangular pattern formed by the extrusion printing of silver ink electrodes. For this approach, we made a water-insoluble and jettable PEDOT:PSS ink by incorporating dodecylbenzene sulfonic acid (DBSA) and the cross-linking agent GOPS. Finally, we used a conductometric method to follow the changes in the resistance of the sensing material, obtaining a linear relationship with indirect proportionality to the temperature.

Harnessing the sensitivity of these materials allows accurate real-time temperature recording. The enhanced stability of PEDOT:PSS due to cross-linking decreases the chance of oxidation by moisture, therefore increasing the longevity of sensor efficacy.[21] This research not only highlights the challenges in sensor innovation but also paves the way for future applications for revolutionizing medical diagnostics, fitness tracking, and health monitoring.

Methodology

Materials

For the substrates, knitted 100% polyester fabric was commercially sourced, and plain microscope glass slides were purchased from Technologist Choice. The sensor on the glass substrate stands as the benchmark sensor for comparison purposes with the wearable sensor. Ethylene glycol (EG) and 1.3% w/v PEDOT:PSS were purchased from Sigma–Aldrich, while GOPS and DBSA were purchased from Fisher Scientific. Finally, the silver ink (120-07) was purchased from Creative Materials Inc.

PEDOT:PSS-EG-DBSA-GOPS ink preparation

For the preparation[25] of ink used in the gap space between the extrusion-printed silver electrodes (called the channel from here on), 1 wt% EG and 0.1 wt% DBSA were incorporated into a commercial 1.3 wt% PEDOT:PSS aqueous solution to enhance ink morphology and jettability, respectively. Additionally, 1 wt% of GOPS was used to cross-link the PEDOT:PSS films, making them water-insoluble, a crucial characteristic for the herein developed temperature sensor. These modifications enhance the hole and ion conductivity of the semiconductor layer between the channels. Finally, prior to its deposition, the ink was filtered to remove any particles formed by agglomeration. The viscosity of this ink was assessed at room temperature using a RheoSense VISC Portable Viscometer (RheoSense Inc., San Ramon, CA).

Sensor preparation on glass and fabric

First, the silver electrodes for the glass substrate were printed using the extrusion printing method as follows. The design for

the printing pattern was created using Autodesk's EAGLE software. A desktop printed circuit board (PCB) printer, specifically the Voltera V-One PCB Printer (Voltera, Kitchener, ON), was used for extrusion printing. The electrical resistivity of the printed silver tracks is 2.5×10^{-5} Ω cm. The extrusion printing was done using a nozzle sized 420 μm. Additionally, a low-sintering-temperature soldering paste (below 205 °C) from Voltera was utilized to attach copper wires to the silver electrodes. For the polyester fabric, Ag threads were sewn as the electrodes, mimicking the channel obtained from the printing process for the glass substrate.

The modified PEDOT:PSS ink was printed in a rectangular shape on both substrates, glass and polyester fabric, using a custom-built piezoelectric drop-on-demand (DOD) inkjet printer, assuring printing on the channel areas. The key printing parameters we employed for the PEDOT:PSS ink were as follows: the printing speed was set to 10 000 μm s^{-1}, a value optimized to ensure stable jetting and precise droplet formation during the process. The drop spacing was carefully chosen to promote uniformity, with 65 μm spacing for line printing and 30 μm spacing between lines when forming rectangular patterns. For the printed PEDOT:PSS patterns, a single layer was applied on glass substrates, while three layers were printed on fabric substrates, with each layer dried at 120 °C for 20 minutes on a hot plate between prints. These parameters were essential for achieving stable jetting, precise patterning, and the desired electrical conductivity, ultimately ensuring the quality and reproducibility of the printed structures for wearable electronics applications. A LabVIEW program (National Instruments, Austin, TX) controlled the printing process, allowing any design to be created by moving the printer stage relative to the printhead. The nozzle (MJ-ATP-01-60-8MX, Microfab Technologies, Inc., Plano, TX) had a 60 μm orifice diameter. The gap distance between electrodes on glass and fabric was 1 and 5 mm, respectively. The width of electrodes on the glass substrate was 1 mm and the length was 1.5 cm, while the thickness of the silver thread as conductive electrodes on the polyester fabric was 0.2 mm, and the length was 1.5 cm.

Characterization

Field Emission Scanning Electron Microscopy (FE-SEM) images were collected on a Quanta FEG 250 without gold sputtering. In our experimental setup to measure temperature-dependent resistance changes, we utilized a Keithley 2400 SourceMeter. Measurements were taken at one-second intervals to capture the dynamic response of the sensors. We positioned our samples—modified PEDOT:PSS printed on glass and polyester fabric substrates—on a precisely controlled hot plate. To ensure accuracy in temperature measurement, a PCT2075 temperature sensor, connected to an Arduino, was placed adjacent to the test sensor to validate the temperature set by the hotplate and for comparison purposes. This setup allowed us to monitor temperature variations with an accuracy of 0.1 °C, as the temperature gradually increased from ambient temperature (23 °C) to body temperature (39 °C). This

methodology not only provided real-time resistance data but also ensured that both substrates were subjected to uniform thermal conditions, facilitating a direct comparison of their performance under identical environmental stresses.

As previously explained, the developed sensor is based on a conductometric approach. To assess the resistance changes, an LM334 chip was employed to provide a constant current through the sensor, thereby ensuring its operation within the desired temperature range. The voltage across the sensor was subsequently measured using the analog-to-digital converter (ADC) of a microcontroller. This measured voltage, in conjunction with the known constant current, enabled the calculation of the sensor's resistance using Ohm's law. By maintaining a constant current, the voltage measurement directly correlated with the sensor's resistance, facilitating the accurate determination of temperature fluctuations. Finally, a polyimide film (Kapton®) was placed on top of and under the fabric sensor to improve stability.

Results and discussion

The ink preparation played a key role in determining the performance of the final sensor, particularly when applied to a fabric substrate. As shown in Fig. 1, PEDOT:PSS was used as the base material due to its well-documented conductivity and applications as a temperature sensor.[16]

When tailored for use on fabric, the formulation of the ink and its interaction with the substrate had a significant impact. In Fig. 1(a), the active material, situated between two polyimide sheets, forms the core sensing layer. These polyimide sheets are essential, as they provide a protective barrier that helps extend the sensor's active lifespan by shielding the PEDOT:PSS from environmental factors. To further enhance the ink's performance, DBSA was added. This anionic surfactant improved conductivity by detangling the PSS chains from the PEDOT backbone, as illustrated in Fig. 1(b).[32]

This detangling process was particularly effective for the fabric substrate, as it allowed for the formation of PEDOT-rich pockets, which significantly boosted the material's conductivity. Ethylene glycol was another critical additive. It influenced the crystallinity of the PEDOT:PSS, encouraging a more ordered structure that improved carrier transport. This effect was especially evident on the fabric substrate, where the ink exhibited better electrical performance than other surfaces like plastic or glass.[32] There were no noticeable differences between the printed films on fabric and other substrates. However, due to the porous nature of the fabric, we anticipate enhanced long-term stability and improved processability. To address potential delamination, GOPS was added as a cross-linking agent. This proved to be an effective solution, particularly for the fabric substrate, where maintaining strong adhesion is challenging. GOPS ensured that the active material stayed in place, even under mechanical stress, and reduced issues seen with delamination on other substrates such as plastic.[32] Overall, these modifications underline the impor-
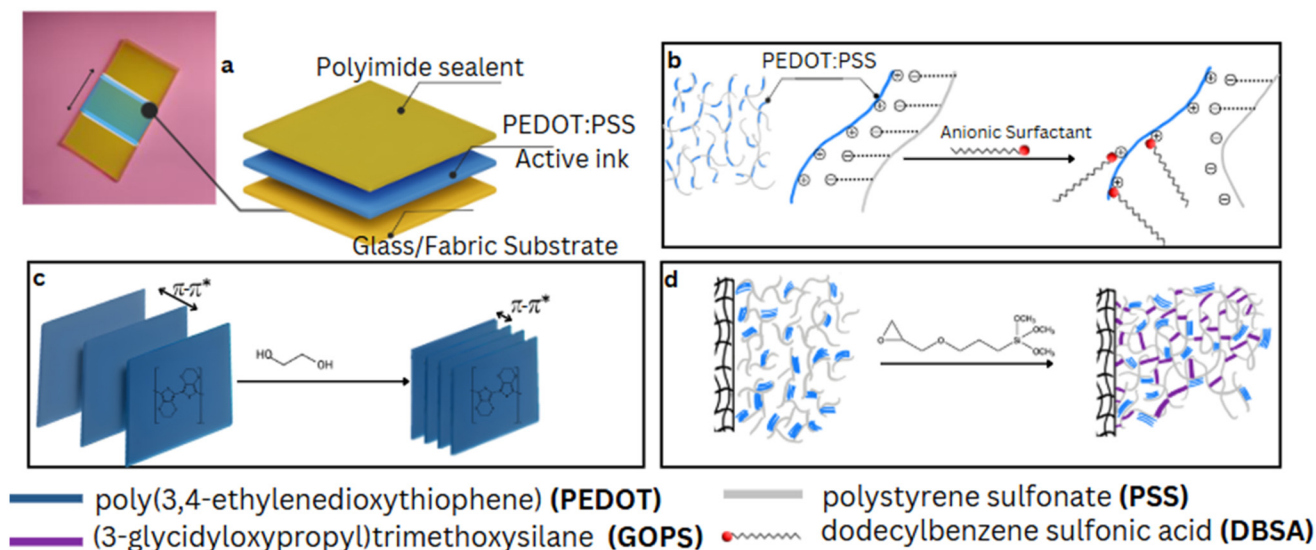
Fig. 1 (a) General scheme and components of the sensor developed herein, (b) effect of DBSA molecules on PEDOT:PSS, (c) effect of ethylene glycol on the PEDOT:PSS polymer, and (d) effect of GOPS as a crosslinking agent in the ink.

tance of fine-tuning ink formulations to suit the specific needs of fabric substrates. By doing so, we achieved a sensor that not only performed well in terms of sensitivity and accuracy but also demonstrated durability and stability, both of which are critical for wearable applications.

Printing process

Fig. 2(a) shows the final temperature sensor with extrusion-printed silver electrodes and inkjet-printed modified PEDOT:PSS in the channel between the electrodes. Fig. 2(a) shows an optical microscopic image of the silver electrode and the PEDOT:PSS-based ink layer.

As observed, the ink is evenly distributed on the glass, with a distinctive interface that covers the edge of the silver electrodes. On the other hand, Fig. 2(b) shows the fabric substrate, in which the expected rough surface is observed; this has the potential to improve the adhesion of the film. The electrical sheet resistance measured for the printed electrodes on glass after 30 minutes of curing at 120 °C is 0.03 Ω sq^{-1}. The normalized resistance (R/R_0, where R represents the instantaneous sensor resistance and R_0 denotes the initial resistance at ambient temperature) of the PEDOT:PSS-EG-DBSA-GOPS-based temperature sensor is plotted over time in Fig. 3(a), showing the inverse directionality of the sensor with temperature.

In the graph, the temperature increased from room temperature (RT) 23 °C to 39 °C gradually on a hot plate, and was then allowed to cool down, while the resistance was recorded over time. Fig. 3(a) shows a decreasing trend when the temperature is increased, reaching the lowest value at 39 °C, with an overall ~30% variation. Fig. 3(b) shows the sensitivity of the sensor considering the heating range (23 °C to 39 °C) by plotting the response variation of the sensor ($\Delta R/R_0 = (R - R_0)/R_0$) versus temperature. It shows ~30% change in resistance for a temperature change of ~16 °C (from RT to 39 °C) and sensitivity of more than 1.7% per °C. The observed variation in resistance with temperature exhibited a linear relationship, evidenced by a determination coefficient (R^2 value) of 0.995, which indicates a strong linear correlation between the sensor's response and temperature. Fig. 3(b) shows that the resistance of the samples decreased as the temperature increased, indicating a negative temperature coefficient (NTC) of resistance. Similar NTC properties have been reported for PEDOT:PSS-based polymer composites in previous studies.[32] In general, for the sensors reported herein, an increase in
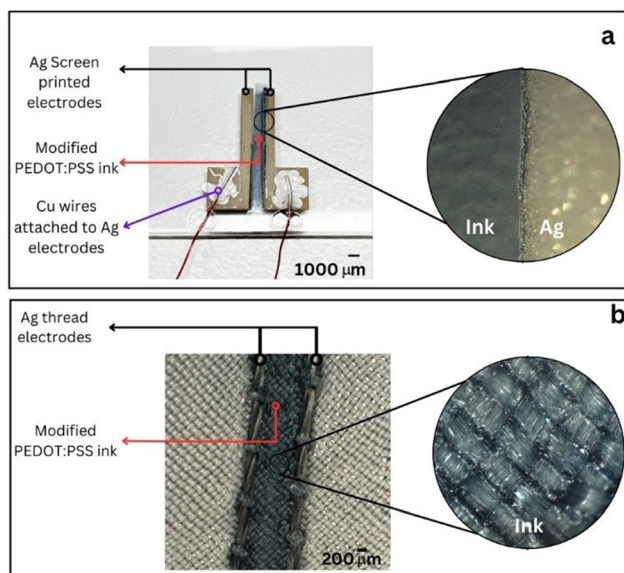

Fig. 2 (a) Temperature sensor on glass with extrusion-printed electrodes and inkjet-printed PEDOT:PSS ink, and (b) the temperature sensor on fabric using Ag threads as electrodes.
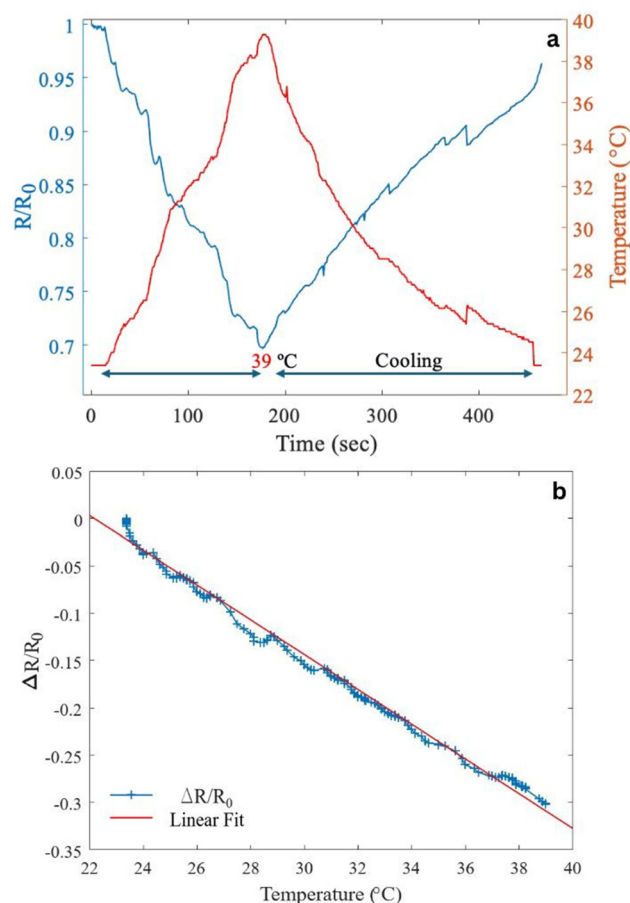
Fig. 3 (a) Normalized resistance of the temperature sensor on glass *versus* time for one heating and cooling cycle and (b) sensitivity of the sensor with temperature and a linear fit to the results.
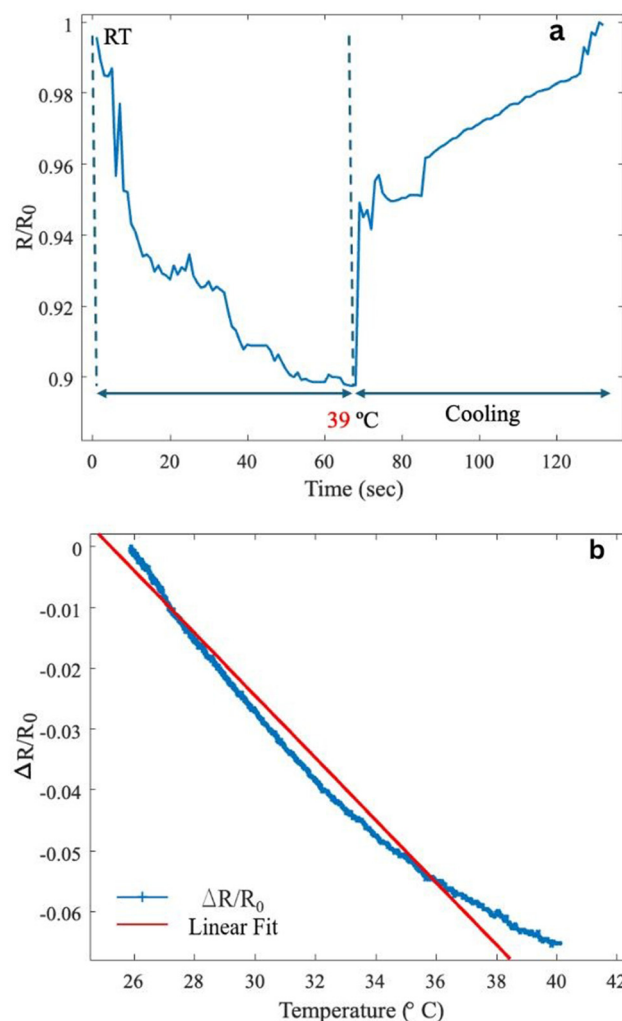

Fig. 4 (a) Normalized resistance of the temperature sensor on fabric *versus* time for one heating and cooling cycle and (b) sensitivity of the sensor with temperature and a linear fit to the results.

temperature can either increase the charge carrier density and/ or their transport. Once the material portion and mixture ratio were optimized on glass, it was deposited on a polyester-based fabric with silver conductive yarn sewn as the electrode, with a gap distance of 5 mm, which is 5 times larger than the gap distance for printing, to avoid short-circuiting, since the frays from the conductive threads can limit the precision of the gap distance. The PEDOT:PSS-EG-DBSA-GOPS was dried and cured on a hot plate at 120 °C for 30 minutes. To test the fabric-based temperature sensor, the temperature was gradually increased from ambient temperature to 39 °C using a hot plate, and the resistance was monitored over time, displaying a trend of decreasing resistance with a variation of approximately 10% over the measurement range (20% less than the glass-based temperature sensor). Fig. 4(a) illustrates the heating and cooling trend of the fabric-based temperature sensor, showcasing its reversibility.

As the temperature rises to 39 °C, the normalized resistance decreases, reflecting the expected response of the sensor to increasing temperature. This is followed by a cooling phase, during which the normalized resistance gradually returns to its initial value as the temperature drops back to room temp-

erature. The consistent return to the baseline resistance value after cooling indicates good reversibility and stability of the sensor's temperature-sensing performance, a critical factor for reliable and repeatable measurements in wearable applications. Fig. 4(b) illustrates the sensor's response variation ($\Delta R/R_0 = (R - R_0)/R_0$) as the temperature rose from room temperature to 39 °C. Considering the temperature range (similar to before), the calculated sensitivity is 0.65% per °C. This represents an enhancement in sensitivity compared to previously reported textile-based temperature sensors,[27–31] which typically demonstrate sensitivities below 0.65% per °C. The resistance change with temperature showed a semi-linear pattern, confirmed by a determination coefficient (r^2 value) of 0.779, which indicates the sensor's linear response to changes in temperature. The nonlinearity observed in the fabric-based temperature sensor could be attributed to the structural differences between the fabric and the glass substrate. Unlike glass, which offers a smooth and uniform surface, fabric substrates have a

porous structure with varying depths due to the fibers and holes in the material. This unevenness makes it challenging to achieve a uniformly deposited active layer, resulting in variations in layer thickness across the substrate. On glass, the active layer is typically more uniform, leading to a better thermal distribution and more consistent temperature gradients within the channel between the two conductive electrodes. In contrast, the irregularities on the fabric substrate can cause localized temperature variations, disrupting the uniform thermal profile needed for linear sensor behavior. These factors collectively contribute to the sensor's nonlinear response when fabricated on fabric substrates. For comparison purposes, Fig. 5(a) highlights the response characteristics of both the textile temperature sensor presented herein and an off-the-shelf reference temperature sensor during thermal cycling tests. In detail, on the *x*-axis is time in seconds, while the *y*-axis tracks the normalized resistance ratio (R/R_0) and the temperature simultaneously. Fig. 5(a) shows the comparison of the response of the textile-based temperature sensor (blue curve) with that of a reference sensor (red curve) during multiple heating and cooling cycles. Both sensors were subjected to identical conditions on the same hot plate. The textile sensor demonstrates a similar time response as the reference sensor, taking 56 seconds to cool from 39 °C to 24 °C, compared to the reference temperature sensor, which requires 59 seconds for the same temperature range. This result highlights the textile sensor's efficiency in responding to temperature changes, showcasing its potential for real-time temperature monitoring. The close agreement between the responses of the two sensors further validates the performance and reliability of the textile-based sensor. Fig. 5(b) shows the stability of the textile-based temperature sensor over 10 days by tracking its resistance at a constant temperature of 36 °C. The resistance shows a gradual increase, with a total change of approximately 13% over the 10-day period. This relatively small increase in resistance highlights the sensor's stability and durability over time, which is critical for its application in wearable devices. The consistent trend and minimal drift in resistance suggest that the sensor maintains reliable performance under prolonged use at a fixed temperature.

Fig. 5(c) illustrates the Relative Change Ratio (RCR) of the sensor under different mechanical deformations, including bending inward, bending outward, and stretching. Despite the application of these mechanical stimuli at specific time intervals (highlighted with dashed vertical lines and corresponding images), the RCR remains within a narrow range (±0.01), demonstrating minimal fluctuation. This indicates that the sensor maintains signal stability under moderate bending and stretching, confirming its mechanical robustness and suitability for wearable applications where dynamic movements are expected.

The morphological stability of the sensor was further characterized using FE-SEM. Fig. 6 shows various stages of the temperature sensor as well as bare fabric fibers. All images were collected without Au sputtering to obtain the fine structure of the surface. Fig. 6(a) shows a fresh sensor, in which the
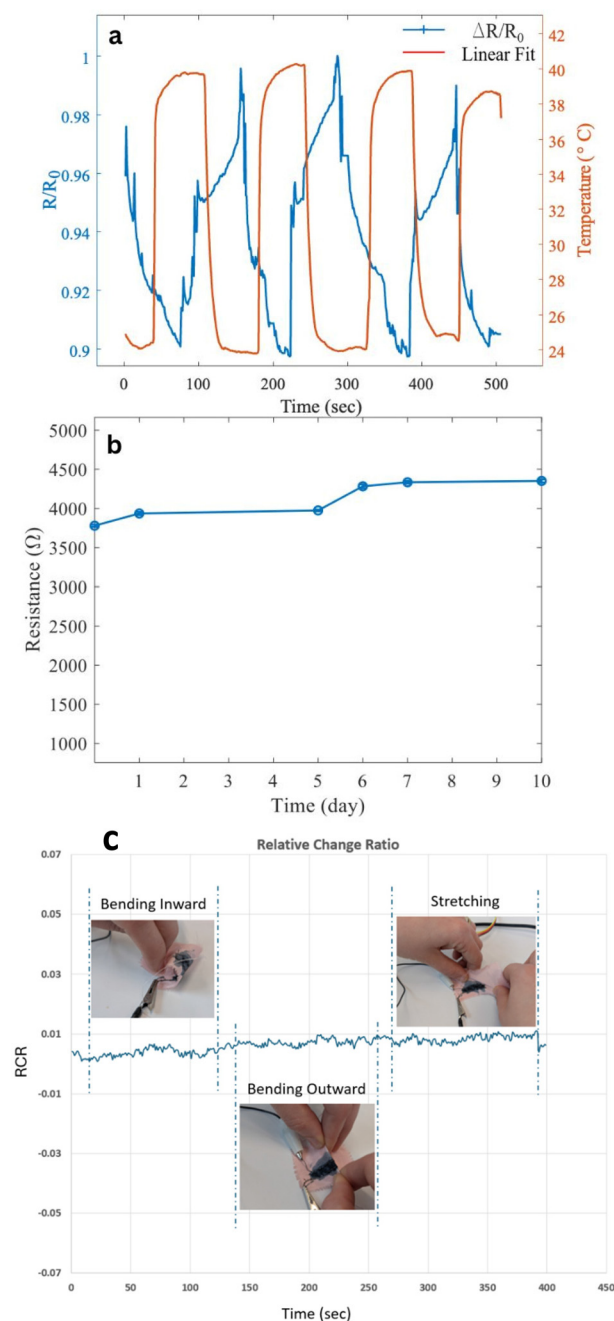

Fig. 5 Dynamic response of the sensor showing R/R_0 and reference temperature over multiple cycles. (b) Long-term stability at 36 °C over 10 days, with a 13% resistance increase due to fabric stretching. (c) Relative Change Ratio (RCR) of the sensor under bending inward, bending outward, and stretching.

fibers are coated with conductive ink, hence providing a less-charged image. On the other hand, after two months of storage the sensor was imaged again to assess the effect of time on the sensor's surface, as observed in Fig. 6(b). It is important to mention that even though the preparation of the ink purposely included a cross-linking agent to stabilize the sensor's performance and the active material stability (GOPS),
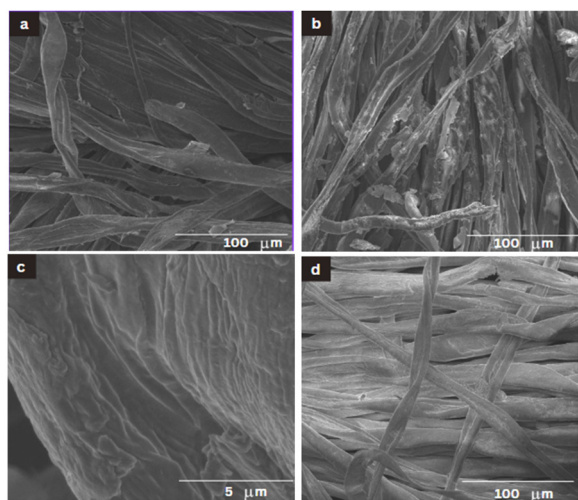
© 2025 The Author(s). Published by the Royal Society of Chemistry

RSC Appl. Polym., 2025, **3**, 1474–1481 | **1479**

Fig. 6 SEM images of a (a) fresh temperature sensor, (b) sensor after 2 months of storage, (c) detailed view of active material folds, and (d) bare fabric fibers. Increased surface charging and delamination over time correlate with sensor resistivity increase.

after some two months of storage time, the presence of a particulate solid is observed. The details on the surface can be further observed in Fig. 6(c), in which the presence of the active material is clearly observed as folds on the threads. Finally, and for comparative purposes, Fig. 6(d) shows the charged fibers from bare fabric. In the micrograph, an increase in charging and delamination is observed, which can be the structural cause of the increase in the resistivity of the sensor observed from 4 kΩ to 10 kΩ when fresh to 2 months old.

As explained before, it is expected that with the increase in temperature, the charge carrier (holes in this case) transport within and between PEDOT grains improves, resulting in a lower resistance. After some time, even with the presence of Kapton® tape to help stability, the changes in the structure of the ink can break this continuum of PEDOT pockets, increasing the resistance over time until the point of failure.[16]

Conclusions

A potential wearable temperature-sensitive sensor was formulated and tested on glass and fabric substrates by implementing PEDOT:PSS ink and silver electrodes. The PEDOT:PSS base allows for increased conductivity and long-term stability of the temperature sensor. When heated on a glass substrate, the resistance change was about 30%, along with a sensitivity of over 1.7% per °C when comparing two temperatures with a difference of about 16 °C. The relationship between resistance and temperature exhibited a linear response of $r^2 = 0.995$, proving that the increase in temperature resulted in the decrease in resistance and an increase in conductivity. Testing on the fabric substrate showed a 10% decrease in resistance, along with a sensitivity of over 0.65% per °C, which, when compared to existing literature, represents a significant enhancement in the

temperature coefficient of resistance (TCR) performance for textile-based sensors. Previous studies have reported TCR values ranging from 0.1% to 0.5% per °C for fabric sensors utilizing conventional materials and fabrication techniques.[27,28,31] The relationship between resistance and temperature exhibited a semi-linear response of $r^2 = 0.779$ and an indirect proportionality, similar to that of the glass substrate. The cooling phase response time was about 56 seconds, which proved similarities between the reference (59 seconds) and the fabric sensor. The performance of the fabric sensor overall has proven to be highly responsive and adaptable to any temperature change. The evidence attested the viability of the fabric sensor; however, further aging showed an increase in resistance over 13% after 10 days, and a 2.5 times increase in the resistance after 2 months. Over time, even with the aid of GOPS for stability, the structure of the ink will continue to break down until failure. Although further investigation into the optimization of the temperature sensor is needed to increase longevity and stability, this will allow its use for multiple future applications, such as daily, sporting, or medical use.

Conflicts of interest

There are no conflicts to declare.

Data availability

The data supporting this article have been included as part of the ESI.†

Acknowledgements

References

1 G. Shin, M. H. Jarrahi, Y. Fei, A. Karami, N. Gafinowitz, A. Byun, *et al.* Wearable activity trackers, accuracy, adoption, acceptance and health impact: A systematic literature review, *J. Biomed. Inf.*, 2019, **93**, 103153.

2 J. Longhini, C. Marzaro, S. Bargeri, A. Palese, A. Dell'Isola, A. Turolla, *et al.* Wearable devices to improve physical activity and reduce sedentary behaviour: an umbrella review, *Sports Med.*, 2024, **10**(1), 9.

3 A. Azizan, W. Ahmed and A. H. A. Razak, Sensing health: a bibliometric analysis of wearable sensors in healthcare, *Health Technol.*, 2024, **14**(1), 15–34.

4 N. L. Kazanskiy, S. N. Khonina and M. A. Butt, A review on flexible wearables–Recent developments in non-invasive continuous health monitoring, *Sens. Actuators, A*, 2024, **366**, 114993.

5 G. Min, G. Khandelwal, A. S. Dahiya, S. Mishra, W. Tang and R. Dahiya, Multisource energy harvester on textile and plants for clean energy generation from wind and rainwater droplets, *ACS Sustainable Chem. Eng.*, 2024, **12**(2), 695–705.

6 F. Li, H. Xue, X. Lin, H. Zhao and T. Zhang, Wearable temperature sensor with high resolution for skin temperature monitoring, *ACS Appl. Mater. Interfaces*, 2022, **14**(38), 43844–43852.

7 B. A. Kuzubasoglu, E. Sayar, C. Cochrane, V. Koncar and S. K. Bahadir, Wearable temperature sensor for human body temperature detection, *J. Mater. Sci.:Mater. Electron.*, 2021, **32**(4), 4784–4797.

8 B. J. Holtzclaw, Monitoring body temperature, *AACN Adv. Crit. Care*, 1993, **4**(1), 44–55.

9 P. Dolibog, B. Pietrzyk, K. Kierszniok and K. Pawlicki, Comparative analysis of human body temperatures measured with noncontact and contact thermometers. in *Healthcare*, MDPI, 2022, p. 331.

10 N. Bouzida, A. Bendada and X. P. Maldague, Visualization of body thermoregulation by infrared imaging, *J. Therm. Biol.*, 2009, **34**(3), 120–126.

11 H. Liu, Y. Li, W. Xie, X. Zhou, J. Hong, J. Liang, *et al.* Fabrication of Temperature Sensors with High-Performance Uniformity through Thermal Annealing, *Materials*, 2023, **16**(4), 1491.

12 H. Hermanns, R. Werdehausen, M. W. Hollmann and M. F. Stevens, Assessment of skin temperature during regional anaesthesia—What the anaesthesiologist should know, *Acta Anaesthesiol. Scand.*, 2018, **62**(9), 1280–1289.

13 A. M. Al-Qahtani, S. Ali, A. Khan and A. Bermak, Performance optimization of wearable printed human body temperature sensor based on silver interdigitated electrode and carbon-sensing film, *Sensors*, 2023, **23**(4), 1869.

14 F. Alshabouna, H. S. Lee, G. Barandun, E. Tan, Y. Cotur, T. Asfour, *et al.* PEDOT: PSS-modified cotton conductive thread for mass manufacturing of textile-based electrical wearable sensors by computerized embroidery, *Mater. Today*, 2022, **59**, 56–67.

15 P. Lugoda, J. C. Costa, C. Oliveira, L. A. Garcia-Garcia, S. D. Wickramasinghe, A. Pouryazdan, *et al.* Flexible temperature sensor integration into e-textiles using different industrial yarn fabrication processes, *Sensors*, 2019, **20**(1), 73.

16 Y. F. Wang, T. Sekine, Y. Takeda, K. Yokosawa, H. Matsui, D. Kumaki, *et al.* Fully printed PEDOT: PSS-based temperature sensor with high humidity stability for wireless healthcare monitoring, *Sci. Rep.*, 2020, **10**(1), 2467.

17 J. Qiu, M. K. Idris, G. Grau and G. W. Melenka, Electroluminescent strain sensing on carbon fiber reinforced polymer, *Composites, Part B*, 2022, **238**, 109893.

18 Y. El-Hajj, M. Ghalamboran and G. Grau, *Inkjet and extrusion printed silver biomedical tattoo electrodes. In: 2022 IEEE International Conference on Flexible and Printable Sensors and Systems (FLEPS)*, IEEE, 2022, pp. 1–4.

19 S. Chandrasekaran, A. Jayakumar and R. Velu, A comprehensive review on printed electronics: a technology drift towards a sustainable future, *Nanomaterials*, 2022, **12**(23), 4251.

20 C. S. Buga and J. C. Viana, A Design of Experiments Study on Inkjet-Printed PEDOT: PSS Temperature Sensors, *IEEE Sens. J.*, 2024, **24**(7), 9449–9461.

21 P. O. Osazuwa, C. Y. Lo, X. Feng, A. Nolin, C. Dhong and L. V. Kayser, Surface functionalization with (3-glycidyloxypropyl) trimethoxysilane (GOPS) as an alternative to blending for enhancing the aqueous stability and electronic performance of PEDOT: PSS thin films, *ACS Appl. Mater. Interfaces*, 2023, **15**(47), 54711–54720.

22 X. Fan, N. E. Stott, J. Zeng, Y. Li, J. Ouyang, L. Chu, *et al.* PEDOT: PSS materials for optoelectronics, thermoelectrics, and flexible and stretchable electronics, *J. Mater. Chem. A*, 2023, **11**(35), 18561–18591.

23 X. Zhang, W. Yang, H. Zhang, M. Xie and X. Duan, PEDOT: PSS: From conductive polymers to sensors, *Nanotechnol. Precis. Eng.*, 2021, **4**, 045004.

24 M. Nazeri, M. Ghalamboran and G. Grau, Laser–Induced Graphene Electrodes for Organic Electrochemical Transistors (OECTs), *Adv. Mater. Technol.*, 2023, **8**(17), 2300188.

25 A. M. Khalaf, J. L. Ramírez, S. A. Mohamed and H. H. Issa, Highly sensitive interdigitated thermistor based on PEDOT: PSS for human body temperature monitoring, *Flexible Printed Electron.*, 2022, **7**(4), 45012.

26 A. Håkansson, S. Han, S. Wang, J. Lu, S. Braun, M. Fahlman, *et al.* Effect of (3–glycidyloxypropyl) trimethoxysilane (GOPS) on the electrical properties of PEDOT: PSS films, *J. Polym. Sci., Part B:Polym. Phys.*, 2017, **55**(10), 814–820.

27 Y. Chen, B. Lu, Y. Chen and X. Feng, Breathable and stretchable temperature sensors inspired by skin, *Sci. Rep.*, 2015, **5**(1), 11505.

28 K. S. Karimov, F. A. Khalid, M. Chani, A. Mateen, M. A. Hussain, A. Maqbool, *et al.* Carbon nanotubes based flexible temperature sensors, *Optoelectron. Adv. Mater., Rapid Commun.*, 2012, **6**(1–2), 194–196.

29 M. D. Dankoco, G. Y. Tesfay, E. Bènevent and M. Bendahan, Temperature sensor realized by inkjet printing process on flexible substrate, *Mater. Sci. Eng., B*, 2016, **205**, 1–5.

30 Y. Moser and M. A. M. Gijs, Miniaturized flexible temperature sensor, *J. Microelectromech. Syst.*, 2007, **16**(6), 1349–1354.

31 M. D. Husain and R. Kennon, Preliminary investigations into the development of textile based temperature sensor for healthcare applications, *Fibers*, 2013, **1**(1), 2–10.

32 S. Zhang, E. Hubis, C. Girard, P. Kumar, J. DeFranco and F. Cicoira, Water stability and orthogonal patterning of flexible micro-electrochemical transistors on plastic, *J. Mater. Chem. C*, 2016, **4**(7), 1382–1385.

© 2025 The Author(s). Published by the Royal Society of Chemistry

RSC Appl. Polym., 2025, **3**, 1474–1481 | **1481**